

Accepted Manuscript

Strong influence of intramolecular Si...O proximity on reactivity: systematic molecular structure, solvolysis, and mechanistic study of cyclic *N*-trimethylsilyl carboxamide derivatives

Roland Szalay, Veronika Harmat, János Eőri, Gábor Pongor

PII: S0040-4039(17)30499-9

DOI: <http://dx.doi.org/10.1016/j.tetlet.2017.04.057>

Reference: TETL 48849

To appear in: *Tetrahedron Letters*

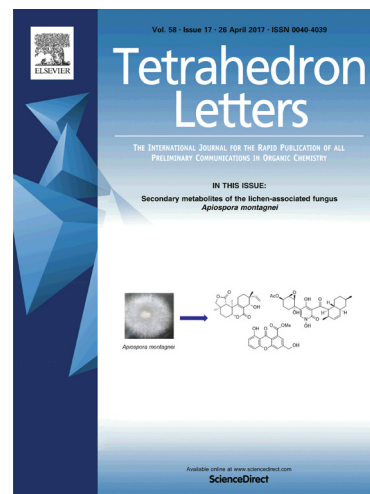
Received Date: 30 January 2017

Revised Date: 12 April 2017

Accepted Date: 18 April 2017

Please cite this article as: Szalay, R., Harmat, V., Eőri, J., Pongor, G., Strong influence of intramolecular Si...O proximity on reactivity: systematic molecular structure, solvolysis, and mechanistic study of cyclic *N*-trimethylsilyl carboxamide derivatives, *Tetrahedron Letters* (2017), doi: <http://dx.doi.org/10.1016/j.tetlet.2017.04.057>

This is a PDF file of an unedited manuscript that has been accepted for publication. As a service to our customers we are providing this early version of the manuscript. The manuscript will undergo copyediting, typesetting, and review of the resulting proof before it is published in its final form. Please note that during the production process errors may be discovered which could affect the content, and all legal disclaimers that apply to the journal pertain.



Strong influence of intramolecular Si...O proximity on reactivity: systematic molecular structure, solvolysis, and mechanistic study of cyclic *N*-trimethylsilyl carboxamide derivatives

Roland Szalay^{a*}, Veronika Harmat^{a,b}, János Eőri^a, Gábor Pongor^a

^a Institute of Chemistry, Eötvös Loránd University, Budapest

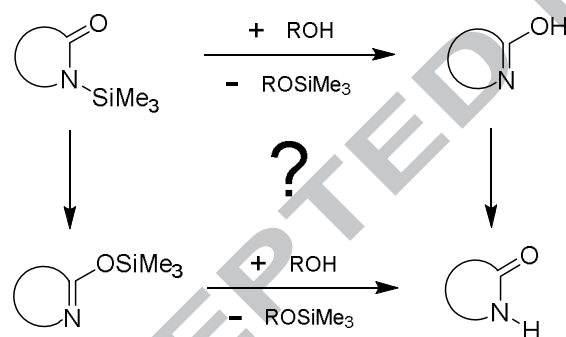
^b MTA-ELTE Protein Modeling Research Group, Budapest

Dedicated to Dezső Knausz for his 80th birthday

Abstract

A comparative alcoholysis study of *N*-silylated derivatives of simple heterocyclic carboxamides (lactams, imides, ureas) is presented. The second-order rate constant values span a range as wide as three orders of magnitude. On the basis of DFT calculations, a good correlation between reactivity and the Si...O distance was found within each family of compounds. The viability of two different reaction pathways was evaluated using a detailed computational mechanistic study of the methanolysis of cyclic urea homologues. Peculiarities in the single-crystal X-ray diffraction structures of the trimethylsilyl and trimethylsiloxy phthalimides are also discussed.

Graphical abstract



Keywords

Silyl; Amide; Solvolysis; Reactivity; Intramolecular; DFT

Introduction

Silylated carboxamide derivatives represent a notable group within organosilicon compounds¹ since they are extensively used as silylating agents for hydrogen-bonded, non-volatile analytes in gas-phase analytical techniques (e.g. gas chromatography and mass spectrometry)² and as protected/activated intermediates in multi-step organic syntheses.³ Moreover, the unsilylated parent compounds (e.g. ureas) have gained increased interest in applications such as organocatalysis and supramolecular chemistry,⁴ hence their controlled release from Si-protected (and lipophilic) precursors by protodesilylation reactions (e.g.

hydrolysis, alcoholysis, fluoride-induced cleavage) under less conventional (e.g. biphasic, phase-transfer catalytic, micelle-forming) conditions may afford novel synthetic routes.⁵

In nucleophilic substitution reactions the increased reactivity of penta- and hexacoordinate silicon atoms over tetracoordinate ones has long been recognized.⁶ One of the first reports concerning the unique reactivity of silylated amides, for example, over silyl amines, was published by Klebe who presumed a switch from the pentacoordinated configuration of the silicon center to the hexacoordinated one upon nucleophilic attack by a proton donor onto the Si atom.⁷ In a later study, Lane and Frye determined the relative thermodynamic silylating abilities of trimethylsilylated *N*-alkyl amides and observed significantly different stability for the silylated pyrrolidone and ϵ -caprolactam, respectively; however this phenomenon was not fully rationalized.⁸

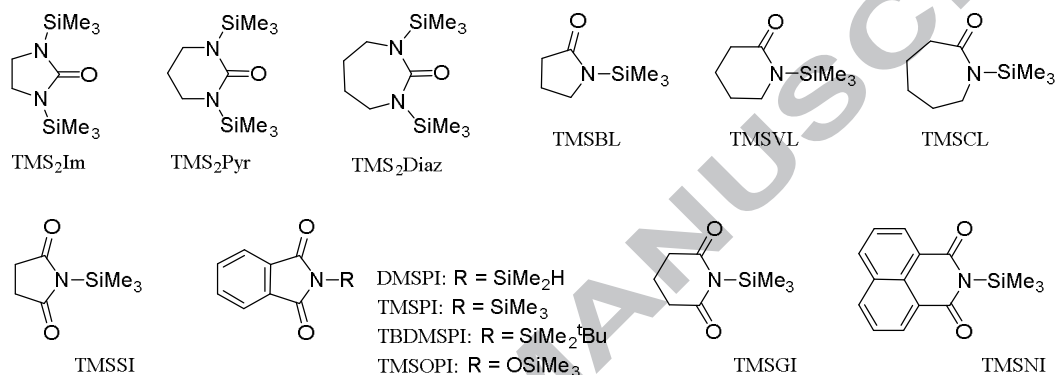
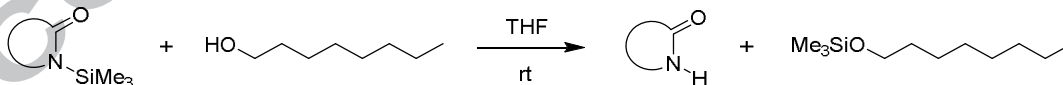


Figure 1. Compounds concerned in this work.

In our previous paper we reported the surprisingly different reactivity of *N*-silylated cyclic ureas with 5- (TMS₂Im), 6- (TMS₂Pyr), and 7- (TMS₂Diaz) membered rings during hydrolysis and alcoholysis reactions.⁹ Both experimental (single-crystal X-ray diffraction) and quantum chemical studies revealed a strong relationship between the ground-state molecular structure of the substrates and their silylating power.^{9,10} Herein, we present an extension of this study relating to silylated cyclic carboxamides, interpreting the new results in a wider perspective (Fig. 1). The octanolysis rate of a series of silyl lactams (TMSBL, TMSVL, TMSCL) and dicarboxylic acid imides (TMSSI, DMSBPI, TMSPI, TBDMSPI, TMSOPI, TMSGI, TMSNI) was determined under similar conditions as previously described⁹ (Scheme 1).



Scheme 1. Octanolysis reaction of silylated cyclic carboxamides.

In order to gain a deeper insight into the ring-size dependent solvolytic reactivity, a detailed computational mechanistic study of the methanolysis of three *N,N'*-disilylated urea homologues (TMS₂Im, TMS₂Pyr, TMS₂Diaz) is also discussed.

Results and Discussion

Syntheses

The silylated lactams (TMSBL, TMSVL, TMSCL) and TMSPI were obtained from the reaction between the corresponding N-H compound and trimethyl chlorosilane in the presence of triethylamine as a proton scavenger. Unlike aromatic (benzene, toluene) or ether (Et₂O, dioxane) solvents commonly used for such reactions,¹¹ CH₂Cl₂ was selected as being one of the best solvents for silylation.¹² DMSPI and TBDMSPI were similarly prepared from phthalimide and dimethyl or *tert*-butyldimethyl chlorosilane. In the case of TMSNI, naphthalimide was first converted into its sodium salt using NaNH₂, then silylated using a THF solution of Me₃SiCl in excess.

Both alicyclic silyl imides (TMSSI and TMSGI) were synthesized by silylation of the corresponding imide with *N,O*-bis(trimethylsilyl)-trifluoroacetamide (BSTFA). Several attempts with commonly used basic silylating agents (e.g. Me₃SiCl/Et₃N, hexamethyl disilazane, trimethylsilyl *N,N*-dimethyl carbamate) failed to give TMSOPI in satisfactory yield since the reversibly formed red-coloured ammonium salt of the deprotonated *N*-hydroxy phthalimide precipitated out of the mixture and therefore could not be efficiently silylated. Using the more powerful reagent BSTFA led to the desired product. To the best of our knowledge, TMSNI and TMSOPI are novel compounds.

Octanolysis study of silylated lactams and imides

Rate measurements were carried out at room temperature in 1-octanol/THF mixtures containing the substrate in 100 times dilution compared to the alcohol. Solvolysis reactions could be conveniently followed using gas chromatography by monitoring the relative peak area of the trimethylsiloxy octane (OctOTMS) formed (Fig. 2).

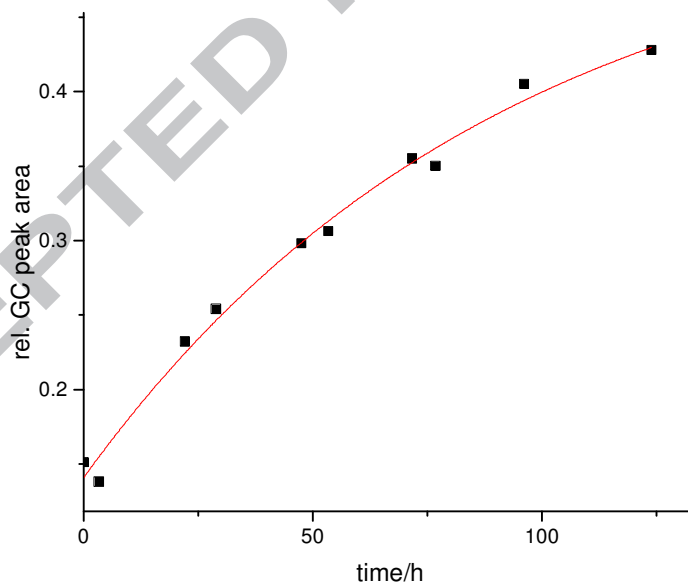


Figure 2. GC peak area of OctOTMS vs time for the octanolysis reaction of TMSPI.

The peak intensity vs time data were evaluated surmising a pseudo-first order kinetic model:

$$X = X_{\infty} (1 - ae^{-k_{\text{exp}}t}),$$

where X , X_{∞} , k_{exp} , t and a denote the actual and final peak area of the OctOTMS (normalised to the internal standard), the pseudo-first order rate constant, the reaction time and a constant parameter, respectively (see the literature for a physical interpretation of the latter parameter⁹). The bimolecular rate constant (k_2) independent of the alcohol concentration was determined in order to characterise the reactivity of substrates where $k_2 = k_{\text{exp}}/[\text{OctOH}]$. Considering the wide range of several orders in magnitude spanned by k_2 s, the $\text{pk}_2 \equiv -\log_{10}(k_2/\text{h}^{-1}\text{mol}^{-1}\text{dm}^3)$ values are instead listed, together with the Gibbs free energies of activation calculated from the Eyring–Polányi equation wherein the transmission coefficient is taken as the unity (Table 1).

Firstly, it should be mentioned, for example, that the difference of $1.7 \text{ kcal mol}^{-1}$ between the $\Delta^\ddagger G$ values for the five-membered (TMSBL) and the six-membered (TMSVL) silyl lactams is reflected in the 16 times faster alcoholysis of the latter compound, whereas the difference of at least $3.4 \text{ kcal mol}^{-1}$ between the corresponding ring-membered silyl ureas indicates a 300 times difference in reaction rates. Upon considering the pk_2 values themselves, it should also be emphasized that even the most reactive compounds examined in this work are not necessarily anticipated to be as efficient as commercially available silylating reagents (e.g. BSA, BSTFA). The original aim of this study was only to show how a slight modification in molecular structure, such as ring expansion remote from the reaction center (Si atom), can influence the silyl transfer capability. On the basis of our results, more efficient and tailor-made silylating agents can be systematically designed, potentially outperforming commonly used reagents.

Table 1. $\text{pk}_2 \equiv -\log_{10}(k_2/\text{h}^{-1}\text{mol}^{-1}\text{dm}^3)$ values for the octanolysis reaction and the Gibbs free energies of activation ($\Delta^\ddagger G/\text{kcal mol}^{-1}$) calculated from the Eyring–Polányi equation (with the transmission coefficient of the unity).

<i>Lactams</i>	pk_2	$\Delta^\ddagger G$	<i>Imides</i>	pk_2	$\Delta^\ddagger G$
TMSBL	4.0	27.8	TMSPI	3.0	26.4
TMSVL	2.8	26.1	TMSSI	2.7	26.0
TMSCL	2.5	25.7	TMSGI	1.9	24.9
<i>Ureas</i>	pk_2	$\Delta^\ddagger G$	TMSNI	0.8	23.4
TMS ₂ Im9	> 3.5	> 27.1	DMSPI	0.6	23.1
TMS ₂ Pyr9	1.0	23.7	TBDMSPI	> 4.0	> 27.8
TMS ₂ Diaz9	1.3	24.1	TMSOPI	2.9	26.3

Secondly, it is apparent from Table 1 (comprising of relevant data for the urea rings for comparison) that there is also a significant but somewhat smaller difference in reactivity between the five- and six-/seven-membered cyclic silylated carboxamides, as was previously reported for silyl ureas. The five-membered rings are less sensitive to nucleophilic attack by the alcohol than their six- or seven-membered congeners; however, in contrast to lactams, the reactivity of the two alicyclic imides (TMSSI and TMSGI) show a diminished dependency upon ring-size. For the six-membered imide ring, a switch from the pure alicyclic skeleton (TMSGI) having only one out-of-plane carbon at the β -position to the all-planar naphthalene-condensed one (TMSNI) significantly enhances the rate of protodesilylation (>10 times). Furthermore, within the series of *N*-silylated phthalimides, the reactivity decreases in the order DMSPI >> TMSPI >> TBDMSPI, corresponding with the increasing bulkiness of the silyl group as expected. The only compound bearing an O-Si bond, TMSOPI, shows a reactivity pattern typical to aliphatic *O*-silylating agents.

Molecular structure studies

In the sense of our simple static (structure-based) model previously developed for predicting the silylating power of *O*- and *N*-silylated carbamic acid derivatives,¹⁰ we explored the relationship between the molecular structure of the title-compounds and their silyl transfer capability, thus providing a starting point to elucidating the detailed mechanism using computational methods (see next section). Out of the five solid compounds, single-crystal X-ray diffraction structures could only be determined for the three phthalimide derivatives (TMSPI, TBDMSPI, TMSOPI; see Fig. 3-5, ESI, and Table 2), mainly due to the extreme moisture-sensitivity of the other two compounds (TMSNI, DMSPI). For all *N*-trimethylsilylated lactams and imides, the ground state equilibrium structures were calculated by quantum chemical (DFT) methods.

In the crystal phase all determined molecular structures are dominated by the largely planar phthalimido moiety. In TMSPI (Fig. 3) the aromatic and five-membered rings, together with their directly attached atoms and the C2 methyl carbon, lie within the crystallographic mirror plane bisecting the C-Si-C angle (C1 Si1 C1) formed by the other two (C1) out-of-plane methyl carbons, thus rendering half of the molecule as the asymmetric unit ($P2_1/m$ space group). The considerably smaller (by 9°) exocyclic C-N-Si angle (C3 N1 Si1) may lead to a more pronounced Si...O interaction between the silicon center and the corresponding carbonyl oxygen (O1). Accordingly, the aforementioned oxygen, together with the in-plane methyl carbon (C2) located on the opposite side represent the quasi apical ligand atoms around a very slightly distorted tetra-to-penta-coordinate silicon center. It is worth noting that based upon examining the Cambridge Structural Database (CSD),¹³ such a significant difference between pairs of the aforementioned angle is unique to *N*-substituted phthalimide derivatives wherein the “isolated” substituent has C_n ($n > 1$) local symmetry (only 4 hits out of 2506 structures). In two of these cases (CSD codes: ICIMAK and IMIGUH) the phthalimido moiety substituent was Sn and one of the three substituents of the tin atom lies within the phthalimido plane, quite similar to the TMSPI structure, suggesting the steric effect discussed below may be effective in Sn-containing analogues. In one of the other two exceptions (CUBJUG), geometric restraints applied for resolving structural disorder might cause the large difference in angles (23.0°), while the other (IMIHIW), is a phthalimido Au complex with the N-Au-X angle being close to 180° . In the crystal all the phthalimido moieties are parallel with the *a*-*c* plane of the unit cell and intermolecular interactions being dominated by aromatic stacking interactions, as well as C-H...O weak, bifurcated hydrogen bonds established by the phthalimido C-H moieties and oxygen atoms not involved in Si...O interactions along the unit cell axis *a*.

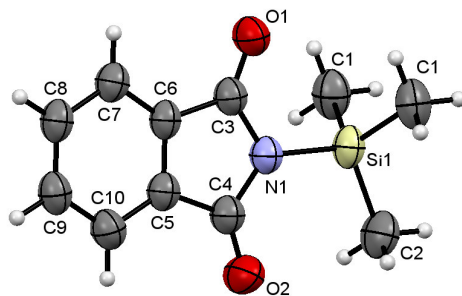


Figure 3. ORTEP drawing of TMSPI at the 30% probability level. Selected interatomic distances [Å] and angles [°]: Si1 N1 1.779(2), Si1 C1 1.801(3), Si1 C2 1.808(4), O1 C3 1.205(4), O2 C4 1.196(4), N1 C3 1.371(4), N1 C4 1.376(4); N1 Si1 C1 107.9(1), C1 Si1 C1 111.2(2), N1 Si1 C2 108.9(2), C1 Si1 C2 110.4(1), C3 N1 C4 108.8(2), C3 N1 Si1 121.0(2), C4 N1 Si1 130.2(2), O1 C3 N1 124.4(3), O2 C4 N1 125.4(3).

Unlike TMSPI, neither TBDMSPI (Fig. 4) nor TMSOPI (Fig. 5) possess a crystallographic mirror plane, however, a quasi-mirror plane perpendicular to the phthalimido skeleton can be fairly defined which is indicated by the close-to-the-right angles ($87.4^\circ/85.8^\circ$) between the C-N-C and the N-Si-C_{tert}/N-O-Si planes, respectively. Furthermore, the latter planes virtually also comprise one more carbon atom since the N-Si-C_{tert}-C/N-O-Si-C torsion angles are anti-periplanar to within $-178.3^\circ/178.0^\circ$ in TBDMSPI/TMSOPI. The crystal packing shows C-H...O weak hydrogen bonds between the phthalimido C-H moieties and oxygen atoms, and C-H... π type interactions between the methyl groups and aromatic rings in both TBDMSPI and TMSOPI. The phthalimido planes of TMSOPI are quasi parallel to the *b-c* plane of the unit cell.

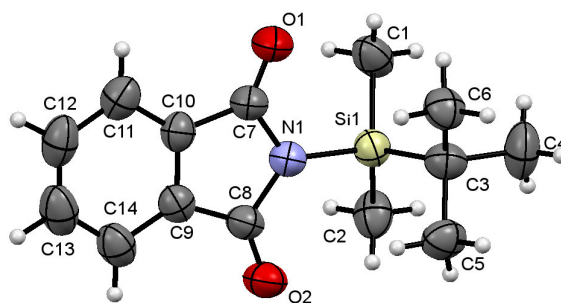


Figure 4. ORTEP drawing of TBDMSPI at the 30% probability level. Selected interatomic distances [Å] and angles [°]: Si1 N1 1.783(7), Si1 C3 1.816(11), Si1 C1 1.838(12), Si1 C2 1.825(11), O1 C7 1.179(9), O2 C8 1.186(8), N1 C7 1.403(9); N1 C8 1.407(9); N1 Si1 C3 106.7(3), N1 Si1 C1 107.8(3), C3 Si1 C1 112.2(5), N1 Si1 C2 107.8(4), C3 Si1 C2 112.9(5), C1 Si1 C2 109.2(4), C7 N1 C8 108.0(6), C7 N1 Si1 124.9(4), C8 N1 Si1 126.9(4), O1 C7 N1 124.2(6), O2 C8 N1 123.8(6).

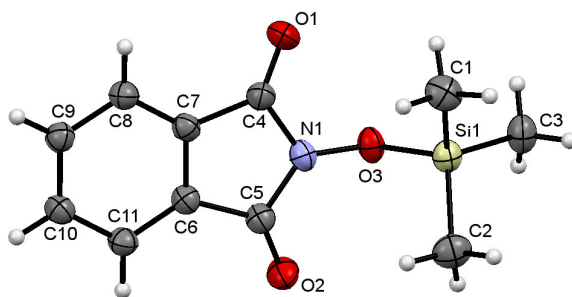


Figure 5. ORTEP drawing of TMSOPI at the 30% probability level. Selected interatomic distances [Å] and angles [°]: Si1 O3 1.703(2), Si1 C3 1.843(3), Si1 C1 1.847(3), Si1 C2 1.844(3), O1 C4 1.192(3), O2 C5 1.199(3), O3 N1 1.387(3), N1 C4 1.400(4), N1 C5 1.403(3); O3 Si1 C3 100.6(1), O3 Si1 C1 110.6(1), C3 Si1 C1 113.2(2), O3 Si1 C2 109.9(1), C3 Si1 C2 112.8(2), C3 Si1 C1 113.3(2), N1 O3 Si1 115.8(1), O3 N1 C4 121.1(2), O3 N1 C5 120.8(2), C4 N1 C5 113.8(2), O1 C4 N1 125.6(2), O2 C5 N1 125.6(2).

Upon comparing the sums of angles around nitrogen (TMSPI: 360.0° , TBDMSPI: 359.8° , TMSOPI: 355.7°), a significant deviance from planarity is observed in TMSOPI, similar to other N-O bonded compounds bearing an amide-type nitrogen. This phenomenon is due to the widely accepted lone pair repulsion between the N and O atoms.¹⁴ Based upon examining the Cambridge Structural Database (CSD), structures with a nitrogen attached to two carbonyl

groups, i.e. dicarboxylic acid imide derivatives, showed the sum-of-angles value of TMSOPI to be the 16th smallest out of the 240 hits. This extent of non-planarity is especially noteworthy in light of the partial delocalization of the O electron density to Si (N-O-Si angle is 115.8°) which might be expected to reduce the stereochemical activity of the oxygen lone pair. Moreover, when taking all *N*-substituted derivatives of phthalimides and their congeners into consideration, the sum-of-angles value for TMSOPI proved to be the 24th smallest out of 4076 hits.

The DFT calculation based (i.e. gas phase) molecular structures exhibit some common features (see ESI). First it should be noted that, due to the extensively conjugated carboxamide moiety and the cyclic connectivity, the molecules are fully, or at least closely flat. Furthermore, in all *N*-TMS derivatives, except for TMSGI, one of the three methyl carbons of the TMS group being farthest away from the oxygen atom virtually lies in the carboxamide plane, similar to the *N*-silylated ureas previously reported. In a steric and stereoelectronic sense, this arrangement of the (C)-Si-N-C=O atoms makes a Si...O interaction (see the literature for a detailed theoretical discussion¹⁰) feasible with some Si-N bond lengthening which is crucial to the silyl transfer ability of substrates. Within the same group of compounds (*N*-silylated lactams, imides, and ureas), a positive correlation is clearly manifested between the higher reactivity (i.e. lower pK_2) in octanolysis and the calculated longer Si-N bond length (Fig. 6), while a similar and even more correlated relationship with opposite sign is shown by the pK_2 vs Si...O distance data points (Fig. 7). These trends provide further evidence to the applicability of our structure-based model previously reported for predicting the silylating power of silylated carboxamide derivatives.¹⁰

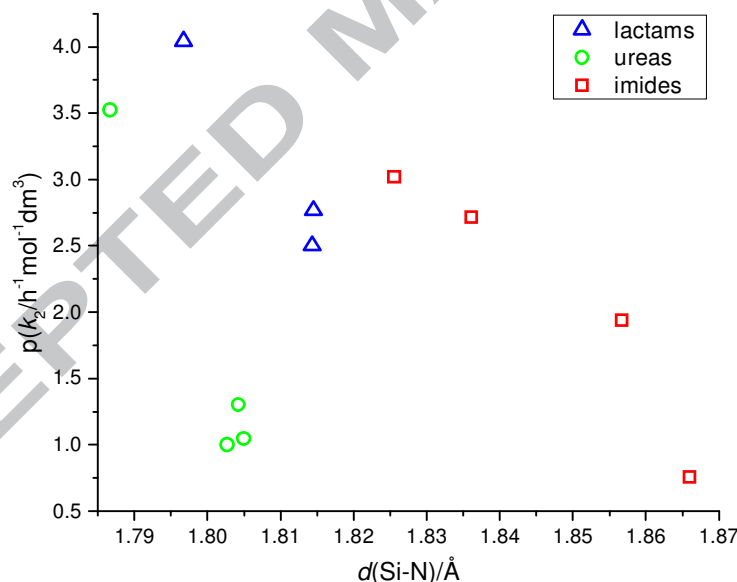


Figure 6. Correlation between pK_2 values for the octanolysis reaction and the Si-N bond lengths in substrates.

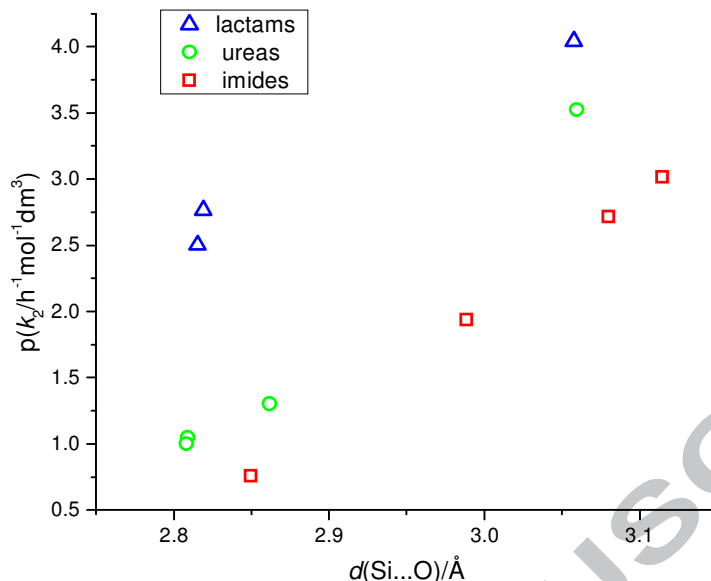


Figure 7. Correlation between $p k_2$ values for the octanolysis reaction and the Si...O distances in substrates.

Computational mechanistic study of the methanolysis of N,N' -disilylated ureas

In nucleophilic reactions of organosilicon substrates, enhanced reactivity of the pentacoordinated silicon over the tetracoordinated one is widely accepted.¹⁵ Previously we reported large differences in the rate of alcoholysis between silylated five- and six-/seven-membered cyclic ureas.⁹ On the basis of our results related to the experimental and theoretical molecular structures, we concluded that the Si atom adopts a more pronounced (pseudo) pentacoordinate geometry in the more reactive six-/seven-membered rings (e.g. TMS_2Pyr , TMS_2Diaz) than in the less reactive five-membered ones (e.g. TMS_2Im). In order to refine and extend our mechanistic view on the alcohol-induced protodesilylation, a detailed picture of the reaction between methanol, for the sake of simplicity, and disilylated cyclic ureas is presented using quantum chemical (DFT) calculations.

Considering the aforementioned close vicinity of the silicon and oxygen atoms, two fundamentally different pathways for the methanolysis reaction can be surmised: (1) the “direct” route *via* a single transition state connecting the MeOH and N,N' -bis(trimethylsilyl) urea molecules directly to methoxytrimethylsilane (TMSOMe) and the enol form of N -trimethylsilyl urea; and (2) an “indirect” two-step route, where an N -to- O silyl migration step occurs in the N,N' -disilylated urea reactant prior to methanol-induced O-Si bond cleavage of the N,O -bis(trimethylsilyl) isourea intermediate which results in the keto form of N -silyl urea beside TMSOMe (Fig. 8-10; for TMS_2Diaz see ESI).

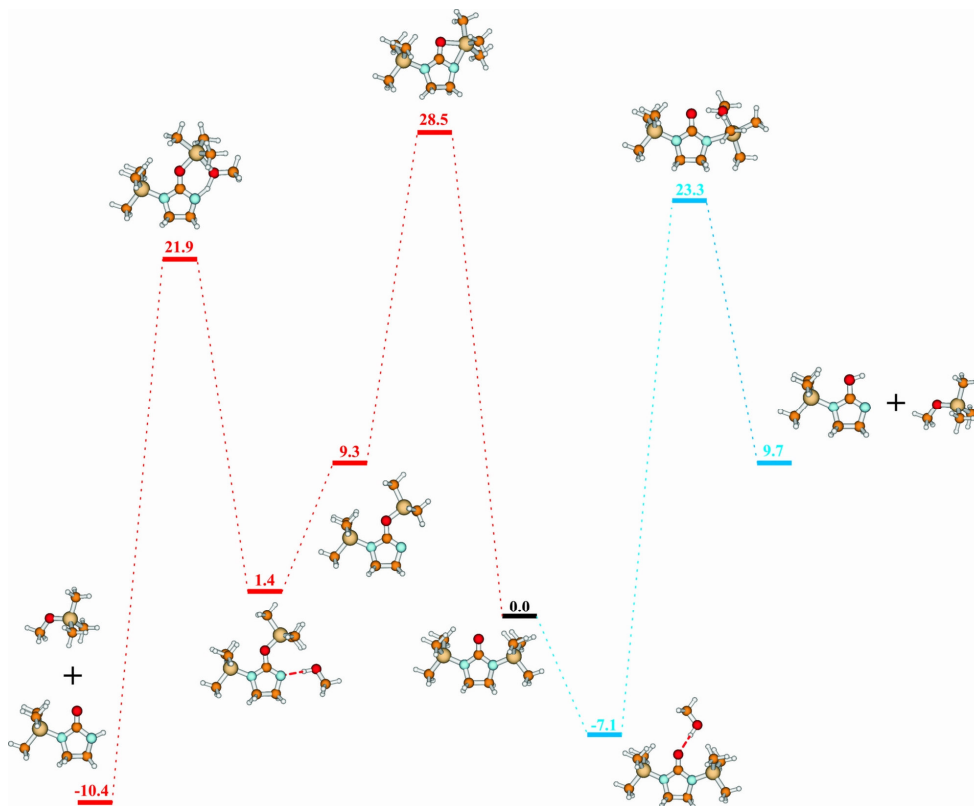


Figure 8. B3LYP/6-31+G* energy profile of the reaction of TMS₂Im with MeOH (Route 1 shown in blue, Route 2 in red). Values are displayed in kcal mol⁻¹.

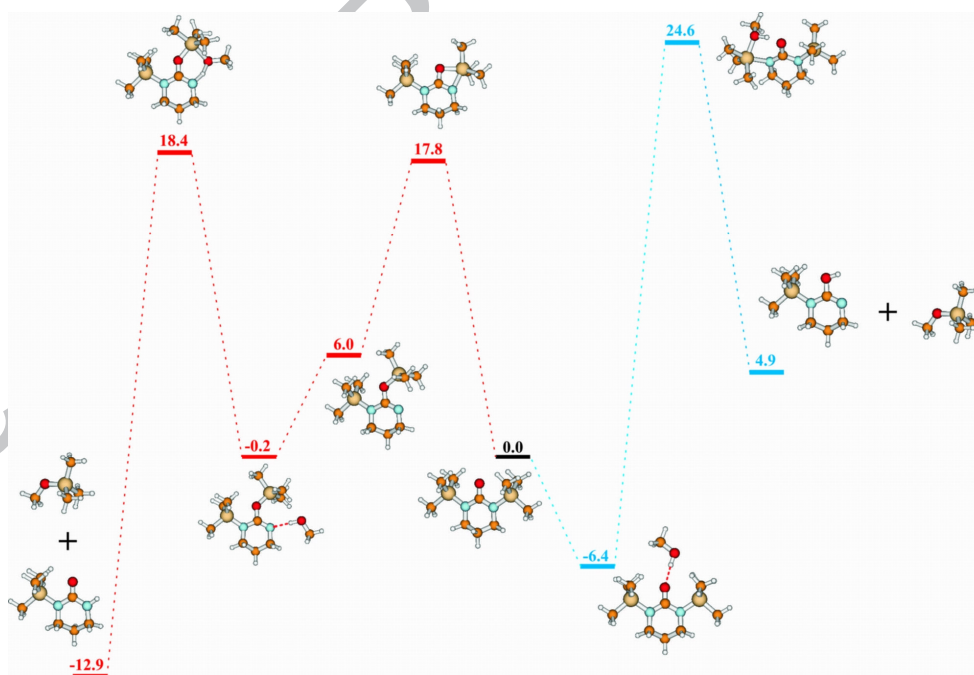


Figure 9. B3LYP/6-31+G* energy profile of the reaction of TMS₂Pyr with MeOH (Route 1 shown in blue, Route 2 in red). Values are displayed in kcal mol⁻¹.

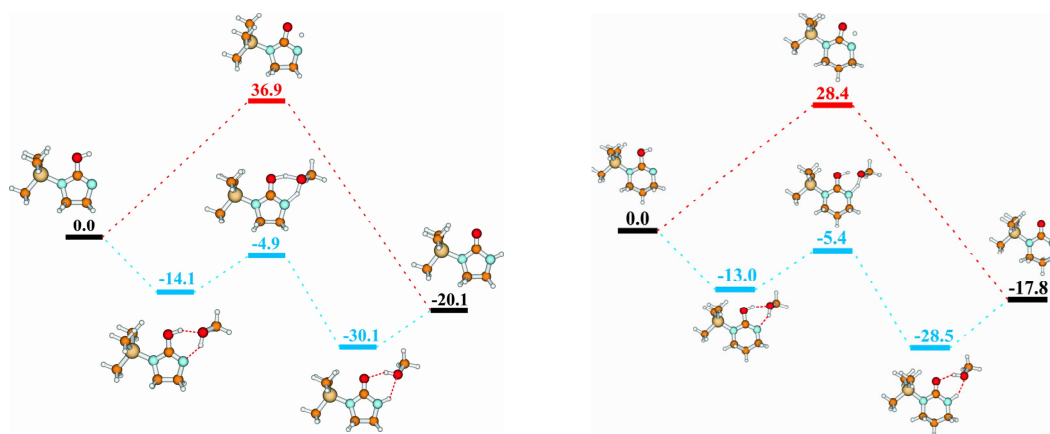


Figure 10. B3LYP/6-31+G* energy profile of the keto-enol tautomerisation reaction of TMS₂Im and TMS₂Pyr (unimolecular pathways shown in red, methanol-assisted pathways in blue). Values are displayed in kcal mol⁻¹.

First, the relative energies of the *N,N'*- and *N,O*-disilylated urea isomers having 5-, 6-, and 7-membered ring were determined. The obtained values show that the latter isomers are less stable in all cases, however, the very close values for 6- and 7-membered rings (6.0 and 5.9 kcal mol⁻¹) are significantly lower than that of the 5-membered ring (9.3 kcal mol⁻¹). During separate calculations concerning the relative stability of monosilylated non-cyclic urea rotamers bearing the Me₃Si-N-C=O moiety, “cis” arrangement of the Si and O atoms was found to be preferable to the “trans” one, and furthermore, the energy gap increased along with a decreasing N-C=O angle. By widening the N-C-N angle due to ring expansion, the prominent strength of the Si-O bond becomes dominant in the 6- and 7-membered rings. Interestingly, in contrast to the discussions above, bond critical point analysis was not able to detect any bond between Si and O even in these higher homologues. For the *N*-to-*O* silyl migration, much higher differences in energy of the relevant transition states were observed between the 5- and 6-/7-membered rings: 28.5 kcal mol⁻¹ for TMS₂Im, and 17.8/15.8 kcal mol⁻¹ for TMS₂Pyr/TMS₂Diaz. These results are in accordance with our structure-based reactivity model which predicts higher silyl group mobility for substrates bearing higher degree of (pseudo) pentacoordination around the Si center (*cf.* TBP% values for TMS₂Im, TMS₂Pyr, and TMS₂Diaz are 5, 20, and 17, respectively).⁹

Complexation of the disilyl urea/isourea substrate with one molecule of MeOH is exothermic (6-8 kcal mol⁻¹) in all cases. The transition states of the Me₃Si-H exchange reaction built-up from the silyl urea-MeOH adduct were determined for both the direct (1) and indirect (2) route. In route 1 the rather high activation barriers (TMS₂Im: 30.4, TMS₂Pyr: 31.0, and TMS₂Diaz: 34.2 kcal mol⁻¹) give little possibility that the reaction proceeds in this fashion, and moreover, the trend in values is opposite to what is expected from the rate measurements. On the contrary, route 2 provides transition states with significantly lower activation energy (TMS₂Im: 20.5, TMS₂Pyr: 18.6, and TMS₂Diaz: 18.4 kcal mol⁻¹), making this pathway much more favourable for the methanol-induced desilylation. These findings are supported by the enhanced silyl transfer ability of *O*-silyl isoureas with the =N...Si-O moiety over *O*-silyl carbamates with the =O...Si-O moiety as previously reported.¹⁰ In sharp contrast to the 6- and 7-membered rings (TMS₂Pyr and TMS₂Diaz), the high barrier of the preceding *N*-to-*O* silyl isomerisation step dramatically reduces the overall reaction rate of the 5-membered cyclic compound (TMS₂Im). In summary, the enhanced reactivity of higher

membered (>5) cyclic *N*-silylated ureas in the desilylation process can be interpreted in terms of the “springboard” role of the carbonyl oxygen acting as an intramolecular nucleophilic catalytic site towards the silicon center.

Conclusion

The structure-based reactivity model previously developed by our group to explain the high silylating power of silyl carbamates, and refined here using a detailed computational mechanistic study of silylated cyclic ureas, proved to be a good starting point to predict the relative rates of silyl transfer reactions for a wider range of substrates. The structural constraints imposed on the accessibility of the carbonyl oxygen for the silicon center play a decisive role in the ease of desilylation. On the basis of the calculated molecular structures, the reactivity of silyl protected/activated intermediates becomes finely tuneable in chemo- and/or regioselective organic transformations which is especially important in the design of highly valuable synthetic targets containing several functional groups.

Acknowledgements

R. Sz. is very grateful to Oldamur Hollóczki for his generous disclosure of computational results relating to the methanolysis reaction. R. Sz. wishes to thank Veronika Kudar and Mária Darvas for their laboratory efforts as undergraduate students, and Zoltán Nyiri for GC-MS measurements. R. Sz. and G. P. acknowledge the OTKA Research Foundation of Hungary F030821 & T037658, and Chemical Works of Gedeon Richter Plc. for financial support.

References

Strong influence of intramolecular Si...O proximity on reactivity: systematic molecular structure, solvolysis, and mechanistic study of cyclic *N*-trimethylsilyl carboxamide derivatives

Roland Szalay^a, Veronika Harmat^{a,b}, János Eőri^a, Gábor Pongor^a

^a *Institute of Chemistry, Eötvös Loránd University, Budapest*

^b *MTA-ELTE Protein Modeling Research Group, Budapest*

Dedicated to Dezső Knausz for his 80th birthday

Highlights

- Wide range of reactivity in alcohol-induced protodesilylation
- Good correlation between reactivity and the Si...O proximity
- Two plausible concurrent reaction pathways
- Noteworthy XRD structural features of silylated phthalimides

¹ Reviews: (a) El Gihani MT, Heaney H. *Synthesis*. 1998; 357-375. (b) van Look G, Simchen G, Heberle J. *Silylating Agents*, Fluka Chemie AG: Buchs, Switzerland, 1995. (c) Wuts, P. G. M. *Greene's protective groups in organic synthesis*, John Wiley & Sons, Inc., Hoboken: New Jersey, 5th ed., 2014.

² Some representative examples: (a) Schettgen T, Dewes P, Kraus T. *Anal Bioanal Chem*. 2016; 408: 5467-5478. (b) Molnar B, Fodor B, Boldizsár I, Molnar-Perl I. *J Chromatogr, A*. 2016; 1440: 172-178. (c) Manzo V, Ullisse K, Rodriguez I, Pereira E, Richter P. *Anal Chim Acta*. 2015; 889: 130-137. (d) Raeppl C, Fabritius M, Nief M, Appenzeller BMR, Millet M. *Talanta*. 2014; 121: 24-29. (e) Cacho JI, Campillo N, Vinas P, Hernandez-Cordoba M. *J Chromatogr, A*. 2012; 1247: 146-153. (f) Kovacs A, Mortl M, Kende A. *Microchem J*. 2011; 99: 125-131.

³ Some representative examples: (a) Homerin G, Baudelet D, Dufrenoy P, Rigo B, Lipka E, Dezitter X, Furman C, Millet R, Ghinet A. *Tetrahedron Lett*. 2016; 57: 1165-1170. (b) Liu GJ, Zhang XT, Xing GW. *Chem Commun*. 2015; 51: 12803-12806. (c) Wahler K, Ludewig A, Szabo P, Harms K, Meggers E. *Eur J Inorg Chem*. 2014; 807-811. (d) Blanck S, Geisselbrecht Y, Kraling K, Middel S, Mietke T, Harms K, Essen LO, Meggers E. *Dalton Trans*. 2012; 41: 9337-9348. (e) Kardon F, Moertl M, Csampai A, Ujszaszy K, Knausz D. *Synth Commun*. 2011; 41: 914-924. (f) Trost BM, Zhang T. *Angew Chem, Int Ed*. 2008; 47: 3759-3761.

⁴ Volz N, Clayden J. *Angew Chem, Int Ed*. 2011; 50: 12148-12155.

⁵ Szalay R. personal note.

⁶ Reviews: (a) Chuit C, Corriu RJP, Reye C, Young JC. *Chem Rev*. 1993; 93: 1371-1448. (b) Wagler, J.; Bohme, U.; Kroke, E. In *Functional Molecular Silicon Compounds I: Regular Oxidation States*; Scheschkewitz, D., Ed.; Springer: New York, 2014, pp 29-105. Some representative examples: (c) Nikolin AA, Kramarova EP, Shipov AG, Baukov YJ, Negrebetsky VV, Arkhipov DE, Korlyukov AA, Lagunin AA, Bylikin SY, Bassindale AR, Taylor PG. *Rsc Adv*. 2016; 6: 75315-75327. (d) Steinhauer S, Stammler H-G, Neumann B, Ignat'ev N, Hoge B. *Angew Chem, Int Ed*. 2014; 53: 562-564. (e) Azhakar R, Ghadwal RS, Roesky HW, Granitzka M, Stalke D. *Organometallics*. 2012; 31: 5506-5510. (f) Metz S, Theis B, Burschka C, Tacke R. *Chem—Eur J*. 2010; 16: 6844-6856. (g) Holloczki O, Nyulaszi L. *Organometallics*. 2009; 28: 4159-4164.

⁷ Klebe JF. *Acc Chem Res*. 1970; 3, 9: 299-305.

⁸ Lane TH, Frye CL. *J Org Chem* 1978; 43: 4890-4891.

⁹ Szalay R, Pongor G, Harmat V, Bocskei Z, Knausz D. *J Organomet Chem*. 2005; 690: 1498-1506.

¹⁰ Pongor G, Kolos Z, Szalay R, Knausz D. *J Mol Struct-THEOCHEM*. 2005; 714: 87-97.

¹¹ Hua DH, Miao SW, Bharathi SN, Katsuhira T, Bravo AA. *J Org Chem*. 1990; 55: 3682-3684.

¹² Knausz D, Meszticzky A, Szakacs L, Csakvari B, Ujszaszy K. *J Organomet Chem.* 1983; 256: 11-21.

¹³ (a) *The Cambridge Structural Database (CSD)*, ver. 5.37. (2016 Feb.). (b) Allen FH, *Acta Crystallogr, Sect B: Struct Sci.* 2002; 58: 380-388.

¹⁴ (a) Mitzel NW, Hofmann M, Waterstradt E, Schleyer PV, Schmidbaur H. *Dalton Trans.* 1994; 2503-2508. (b) Mitzel NW, Angermaier K, Schmidbaur H. *Organometallics.* 1994; 13: 1762-1766. (c) Mitzel NW, Schmidbaur H. *Z Anorg Allg Chem.* 1994; 620: 1087-1092.

¹⁵ Bassindale, A. R.; Glynn, S. J.; Taylor, P. G. In *The Chemistry of Organic Silicon Compounds*; Rappoport, Z.; Apeloig, Y., Eds.; Wiley: New York, 1998, Vol. 2, pp 495-511.

ACCEPTED MANUSCRIPT